 DOI: 10.21608/adjalexu.2023.247149.1439

EFFECT OF BONE MARROW MESENCHYMAL STEM CELLS DERIVED EXOSOMES LOADED IN COLLAGEN HYDROGEL ON BONE REGENERATION IN MALE RAT CALVARIAL CRITICAL-SIZE BONE DEFECT

Sara A. Hamza[1] *PhD* *, Marwa Gamal Noureldin[2] *PhD*, Lamia A. Heikal[3] *PhD*, Enas Magdi Omar[4] *PhD* , Hagar Sherif Abdel Fattah[1,5] *PhD*

ABSTRACT

INTRODUCTION: Expanded bone damage in defects of critical size demands interventions for the complete regeneration. However, limitations of the previous strategies include reduced availability of autograft donors. The therapeutic efficacy of exosomes has been extensively studied in numerous circumstances such as wound healing, bone and periodontal regeneration.

AIM: This research work aimed to test the efficacy of collagen thermoresponsive hydrogel loaded by BMMSC-derived exosomes on bone regeneration in rats' calvarial critical-size bone defects.

MATERIALS AND METHODS: Twenty albino rats were allocated into 2 groups, 10 rats each. Group I- collagen hydrogel (COLL), Group II- (COLL+ exosomes). Calvarial critical-size bone defects were surgically created in all groups. The defects in Group I were filled with collagen hydrogel, and in Group II were filled with exosomes-loaded collagen hydrogel. Rats were euthanized after 4 and 8 weeks, and the calvariae were collected and processed. The regenerated bone was evaluated by histology, histomorphometry, and immunohistochemical expression of the bone formation marker osteocalcin.

RESULTS: Analyzing the new bone using histology and histomorphometry revealed an enhanced quantity and pattern of bone formation in defects augmented with collagen hydrogel loaded by exosomes compared to the bare collagen hydrogel group after 4 weeks. However, after 8 weeks no significant difference was detected between groups. Immunohistochemical expression of osteocalcin showed higher values in group II (Coll + exosomes) in comparison to group I collagen hydrogel (COLL).

CONCLUSION: Bone marrow mesenchymal stem cells derived exosomes loaded collagen thermoresponsive hydrogel provides a precious substitution to cell-based therapy in bone regenerative procedures.

KEYWORDS: Exosomes, collagen thermoresponsive hydrogel, bone regeneration, critical size bone defect, bone marrow-derived mesenchymal stem cells.

RUNNING TITLE: Effect of Bone Marrow Mesenchymal Stem Cells derived Exosomes loaded in Collagen Hydrogel on Bone Regeneration in male Rat Calvarial Critical-Size Bone Defect

1 Oral Biology Department, Faculty of Dentistry, Alexandria University, Egypt.
2 Oral and Maxillofacial Surgery Department, Faculty of Dentistry, Alexandria University, Egypt.
3 Pharmaceutics, Department, Faculty of Pharmacy, Alexandria University, Egypt.
4 Oral Pathology Department, Faculty of Dentistry, Alexandria University, Egypt.
5 Oral Biology Department, Faculty of Dentistry, Beirut Arab University, Lebanon.

* *Corresponding Author:*
Email: sara.ashraf.dent@alexu.edu.eg

INTRODUCTION

Large skeletal defects could result from traumatic fractures, resection of tumors, infections that induce non-restorable bone loss such as progressive periodontitis, or requires bone excision like osteomyelitis, and wounds with significant bone loss such as gunshots [1]. Post-extraction residual ridge resorption causes significant bone loss in the alveolar bone that could not reform naturally [1]. Expanded bone damage in bone defects of critical size demands interventions for the complete regeneration of bone. Traditional reconstruction techniques include autologous graft the "gold standard", allograft, and cells-based therapy alone or associated with human-derived biological materials [2]. However, limitations of the previous strategies include the following: reduced availability of autograft donors and excessive morbidity [1], allograft-related infections, high cost , and risk of immunogenic rejection by the host [3]. Therefore, customized scaffolds mimicking the bony structure, made of bioinspired materials such as collagen and hydroxyapatite crystals "3D bioprinting", have been also developed and accomplished successful bone regeneration combined with proper biomolecules and nanomedicines [1]. Mesenchymal stem cells

(MSCs) were primarily discovered in 1966 by Alexander Friedenstein et al in the bone marrow post-native mammals [4]. Later in 1991, Caplan revealed the pluripotent potential of MSCs to differentiate into, skeletal-tissues forming cells, osteoblasts, and chondroblasts [4]. Compared to embryonic stem cells generated from the embryoblast of the blastocyst, MSC populations are adult stem cells with a limited ability for differentiation [2]. MSC cells are derived from several adult human tissues such as bone marrow, peripheral blood, synovial membrane, adipose tissues, organs (such as pancreas, intestine, and brain), skin and hair follicles, as well as in dental and paradental tissues [2]. Even though MSCs-based tissue engineering has shown considerable potential for bone healing, the achievement of complete and sustainable bone regeneration is still challenging. Reported concerns include the uncontrollable and fast differentiation in vivo, prolonged duration of treatment, potential tumorigenicity [5], and raising ethical conflicts [6]. Moreover, the therapeutic potential of MSC is affected by individual systemic conditions related to metabolic bone diseases, inflammation, hormonal, and immunologic status that hinders their osteogenic differentiation pathway and survival [7].

Recent in-vitro studies clearly proved that MSCs achieve their regenerative outcome through the release of factors, in extracellular vesicles, that promote cellular chemotaxis, migration, proliferation, and differentiation [8]. Exosomes are nanosized extracellular vesicles bounded by a bi-lipid membrane 30-150 nm in diameter [8]. First discovered in 1983 by Rose Johnstone and colleagues, they were found in abundance throughout most body fluids, including blood, saliva, breast milk, urine, cerebrospinal fluid, bile, and lymph [9]. Exosomes, secreted by most cell types and because of their dynamic cell-to-cell interaction, have been involved in various physiological and pathological mechanisms for instance cancer and viral infections [9]. MSCs-derived exosomes act as paracrine mediators responsible for intercellular communication. They could even penetrate target cells and direct their roles as they enclose diverse proteins in the form of receptors, enzymes, transcription factors, lipids, miRNAs, and mRNA molecules. The contained RNA sequence as well as the biological actions of exosomes is highly dependent on the origin of the isolated MSCs [10]. Mesenchymal stem cells could be isolated from the umbilical cord, adipose tissue, bone marrow, amniotic fluid, and dental pulp. The traits of bone marrow-derived mesenchymal stem cells (BM-MSCs) include a reduced risk of infection and rejection, besides a steady biologic behavior [9]. The clinical application of exosome-based therapeutics is suggested to successfully substitute their mother cells and therefore overcome the drawbacks of cell-based strategies [10]. The recent years, the therapeutic efficacy of exosomes has been extensively studied in numerous circumstances such as wound healing, cardiovascular conditions, liver, kidney, and brain diseases, in addition to bone and periodontal regeneration [11]. Furthermore, the transplantation of BM-MSCs derived exosomes in animal models successfully promoted bone regeneration in non-union and rotator cuff reconstruction models as well as calvarial critical-sized bone defects [12].

Bone immunomarkers have been implicated in the detection of bone neo-formation. Osteocalcin is a biochemical marker for bone formation and new bone remodeling in physiologic and pathological conditions [13].

As far as we know, there is not enough information in the literature about the ability of BM-MSCs-derived exosomes loaded in collagen thermoresponsive hydrogel to promote bone regeneration. Therefore, the current work was planned to assess the effectiveness of BM-MSC-derived exosomes loaded in collagen hydrogel on bone reconstruction in rat calvarial critical-size bone defect.

MATERIALS AND METHODS

The present experiment strictly conforms to ARRIVE guidelines (Animal Research: Reporting of In Vivo Experiments) [14]. This current experimental animal research was performed after being approved by the Research Ethics Committee, Faculty of Dentistry, Alexandria University. All procedures followed the institutional and international guidelines for Animal Experimentation and the National Research Council's Guide for the Care and Use of Laboratory Animals. Stem cell processing as well as preparation of exosomes was performed at Center of Excellence for Research in Regenerative Medicine and its Application (CERRMA), Faculty of Medicine, Alexandria, Egypt.

The sample size was computed utilizing the Power Analysis and Sample Size Software (PASS 2020) "NCSS, LLC. Kaysville, Utah, USA, ncss.com/software/pass" The minimum hypothesized sample size total needed to assess the effectiveness of BMMSC- derived exosomes loaded in collagen hydrogel on bone regeneration in rat calvarial critical-size bone defect; was of 20 healthy male adult Wistar albino rats (10 per group) considering significance level of 5%, power of 80% and effect size of 25% using Chi-square test [15, 16].

A total of 22 rats participated in the current study. Two male albino rats 40 grams in weight and 3 weeks of age were used to isolate mesenchymal stem cells. Twenty adult male Wistar albino rats in good health aged from 8-10 weeks and their weight ranged 160-180 grams were incorporated in the experimental procedures. Rats that were involved

in earlier experimental research, and had any ailments, or wounds were excluded. Animals were acclimatized for 2 weeks in the animal house of the faculty of medicine, at Alexandria University before starting the experiment. Cages with bottom wire mesh were used for rat housing under standardized conditions of 12:12 hours a day/night cycles, a temperature (24 ± 2 °C), controlled room humidity with free access to water, and standard diet. Animals were monitored regularly where their activity and ability to freely access food were assessed.

Animals were distributed at random into test and control groups using a random number generator (Prism G. version 5.04, GraphPad Software Inc: San Diego, CA, USA). The allocation sequence/code were blindly allocated to the intervention arms using a sealed opaque envelope. Rats were assigned as follows:

Group I- Collagen group (COLL) (n=10), calvarial critical-size bone defects were surgically created and filled with collagen hydrogel.

Group II- Exosomes loaded collagen group (COLL+ Exos) (n=10), calvarial critical-size bone defects were surgically created and grafted with exosomes loaded collagen hydrogel.

BM-MSCs isolation and culture [17].

Rats' tibias and femurs were dissected aseptically, with the boney ends of the being cut to reveal the interior marrow shaft. With a twenty-three-gauge needle and a five milliliter syringe attached, complete media was injected into a fifty milliliter falcon tube to flush the bone marrow. Flushed out marrow was re-suspended and filtered using a seventy-millimeter filter mesh into a brand new falcon tube to exclude any bony fragments or muscular fibers and cellular aggregates. Centrifugation of the obtained cellular suspension was performed at one-thousand and two-hundreds RPM for five min, followed by resuspension into complete culture media [DMEM Dulbecco's Minimum Essential Medium L.G (Lonza, Belgium)] augmented with ten percent fetal bovine serum (FBS), one-hundred IU mL-1 penicillin and one-hundred mg mL-1 streptomycin (Thermo Fisher Scientific, Waltham, MA)] cultured in T-twenty-five flask and incubated in humidified five percent carbon-dioxide incubator at thirty-seven degree centigrade. After 48 hours, the medium was replaced and the non-adherent cells were eliminated, then replaced every two to three days. At eighty percent confluence level, adherent cells were rinsed two times with phosphate buffer saline (PBS) then 0.25% trypsin/ethylene diamine tetra-acetic acid (EDTA) (Thermo Fisher Scientific, Waltham, MA) solution was used to detach the cells which were split up in a ratio of one to three. The present research MSCs at the third passage (P3). Cultured cells were monitored utilizing a phase-contrast inverted microscope supplemented by a digital camera (Olympus CKX41SF, Japan).

Characterization of Bone marrow-derived mesenchymal stem cells:

BM-MSC Immuno-phenotyping by flow cytometer [18].

Fluorescence-labeled monoclonal antibodies (mAb) were used to characterize P3 BM-MSCs by detecting the surface markers CD11b, CD44, CD45, CD73, CD90 and CD105. Trypsinization of adherent cells was followed by phosphate buffer solution washing and a 30-minute incubation period at room temperature in the dark; with monoclonal phycoerythrin (PE)-conjugated anti-bodies for CD11b, CD44, CD73, CD105 (Abcam, Cambridge, UK), FITC-conjugated antibody for CD45 (Abcam, Cambridge, UK) and mono-clonal Allophycocyanin conjugated antibody for CD90. The cells were washed with phosphate buffered solution three times then re-suspended in 500 µl FACS. Utilizing a BD FACS caliber flow cytometer and Cell Quest software (Becton Dickinson, New Jersey, USA), immunofluorescence was done on live cells.

Preparation of exosomes [17, 18].

BM-MSCs at passage 3 showing 80% confluence, were cultured in serum-free media for 48 hours. Thereafter, EVs were prepared for isolation after the conditioned media was collected. The conditioned serum-free medium was first centrifuged at 300 x g for five min at room temperature to get rid of any cell debris. After a second high-speed centrifugation of the supernatant at 3000 x g for 40 min at room temperature to eliminate large micro-vesicles, the supernatant was filtered through a 0.2um filter. To isolate EVs (50–500 nm), ultracentrifugation (Thermo Fisher Micro Ultracentrifuge MX 120þ) was done at 120 000 x g 4ºC for 70 min. The pellet was suspended again in PBS and divided into aliquots and stored at -80 ºC for further quantification, characterization, and loading to the collagen hydrogel.

Characterization of Exosomes

a.Zeta-sizer (Malvern, UK)

The size of isolated exosomes and their polydispersity index (PDI) was measured using a Zetasizer Nano ZS90 (Malvern Pananalytical, Malvern, UK). Distilled water was used to dilute the samples at a ratio 1:100. Dynamic A laser wavelength 633 nm and 90◦ scattering angle at 25 ◦C was utilized to perform light Scattering.

b. Transmission electron microscopy (TEM)

The exosomes pellet was dissolved in PBS, added onto Cu grids, and stained with 1% (w/v) Phosphotungstic acid (PTA). Samples were then inspected by TEM (JEOL JEM-1400 plus, Tokyo, Japan) and the diameter of the nano-sized vesicles was measured [19].

c.Exosomes quantification using BCA protein assay

Quantification of the exosomes was performed by the total protein content estimation from the isolated

samples utilizing the Bicinchoninic acid (BCA) protein assay kit (Sigma-Aldrich, USA) [18].

Preparation of exosomes-loaded collagen thermo-responsive hydrogel:

Collagen (200 mg/mL in 0.1 M acetic acid solution) and Pluronic acid F-127 (20% w/w) were used to create the collagen thermo-responsive hydrogel. To eliminate air bubbles, the solution was then sonicated for 30 minutes. Beta-Glycerophosphate (10%w/w, G9422, Sigma Aldrich, Taufkirchen, Germany) was then added dropwise to the Pluronic F-127/collagen solution until pH 7.4 was attained and stored at 4oC [20, 21].

For preparation of exosomes loaded collagen hydrogel. The exosomes were added to the Pluronic F-127/Collagen solution then Beta-Glycerophosphate was added as previously explained.

Characterization of thermoresponsive collagen hydrogel:

a) Investigation of Gelation Behavior

The unloaded and exosomes-loaded collagen thermo-responsive hydrogels were assessed for the gelation behavior using the vial tilting method by calibrating gelation time at variable temperatures (4oC, 25oC, and37oC) [20]. Gelation time was recorded at the level where there wasn't any flow for more than one min after frequently up turning the vial with 1 mL gel. The experiment was performed in triplicates.

b) Swelling Ratio (SR)

Collagen thermo-responsive hydrogels with and without exosomes were immersed into de-ionized water at room temperature for 0.5, 1, 6, and 24 hours to determine swelling ratio. By the termination of each incubation period, the hydrogels were washed carefully with deionized water and blot-dried using filter paper after which the weights of the swollen hydrogel were weighed to record the wet weight. The dry weight was considered as the weight of the sample prior to immersion in de-ionized water.

SR was obtained from this equation [20]:

SR = [(Wwet - Wdry)/Wdry]

where Wwet is the hydrogels' final mass following their swelling in deionized water Wdry is the initial mass of the hydrogel samples. All studies were conducted in triplicates.

c) Viscosity measurement:

The viscosity of the prepared unloaded and exosomes-loaded collagen thermo-responsive hydrogels was measured using Brookfield multipoint viscometer at a speed of 1 rpm and spindle CP-40 at 37oC.

Surgical procedures:

All rats received general anesthesia. Their scalps were then shaved and painted with povidone-iodine for disinfection purposes. A midline incision of 2 cm was performed sagittally and the tissues were dissected and reflected using a small periosteal elevator to bare the skull bones bilateral to the sagittal suture. Midway along the sagittal suture, a critical size bone defect of 6mm was created using a trephine drill mounted on a contra-angle handpiece with constant saline irrigation. The drilling was executed cautiously and did not extend to full thickness to preserve the dura matter of the brain from damage. A small diamond round bur was then used to accentuate the depth of the outline in the presence of copious irrigation. Once the defect outline was deep enough, a periosteal elevator was used to elevate the 6 mm calvarial disc, then, irrigation was carefully done to examine the circular defect area and clear the blood (Figure 1a-e) [22].

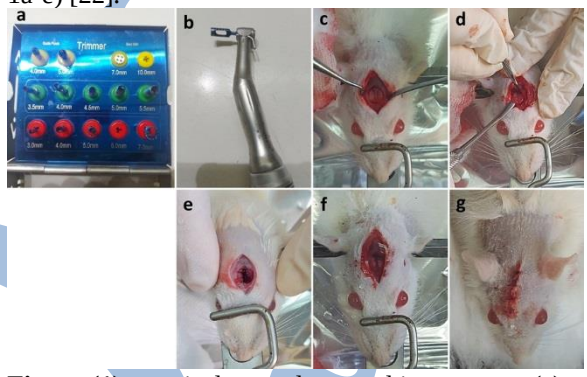

Figure (1): surgical procedures and instruments (a) Kit of different-sized trephine drills,
(b) Size 6mm trephine drill mounted on a contra-angle handpiece, (c) Outline of critical size bone defect of 6mm, (d) Periosteal elevator used to elevate the 6 mm calvarial disc
(e) The brain defect after removal of the calvarial disc, (f) Hydrogel loaded above the brain defects, (g) The incision line sutured using 4/0 vicryl sutures.

For Group I (COLL), the hydrogels were loaded into the created calvarial defects, while for Group II (COLL+Exos) Exosomes-loaded hydrogels were loaded. Immediately, upon gelation of hydrogels, the incision line was sutured using 4/0 vicryl sutures (Figure 1f, g). After that, the rats were transferred to their housing at room temperature and observed for any signs of suffering. Lastly, they were moved to their cages, where they could easily reach food and water. Rats were separated as one rat per cage because the smell of blood may cause rats to harm each other. Any sickness or surgery-related complications were recorded.

Animals euthanasia

After 4 & 8 weeks animals were euthanized by intravenous pentobarbital sodium (Nembutal, Akorn, Illinois, USA) in overdose (120 mg/Kg). The calvaria was dissected out and prepared for light microscopic examination, histomorphometry, and immunohistochemical evaluation. After confirmation of the rats' death, special authorities handled the remains of the rats' bodies.

Histological evaluation

Formalin-fixed calvaria of all rats (n=10 per group), were decalcified, dehydrated, cleared in xylene, then infiltrated and paraffin wax-embedded

into blocks [23]. 4-5µm sections were stained by Hematoxylin and Eosin (H&E) and Trichrome stains. Slides were assessed by light microscope to evaluate the newly formed calvarial bone filling the defect and detect the progression of healing. Photomicrographs X40, 100, and 400 were captured using a digital camera coupled to the microscope (Optika, B-290 series, Ponteranica, Italy).

Histomorphometric analysis

Computer-assisted histomorphometric analysis was conducted by a double-blinded investigator to quantify the surface area percent of newly formed calvarial bone among groups (n=10 per group) [24].

Immunohistochemistry

Immunohistochemical staining was HC staining using Anti- Osteocalcin Rabbit antibody (Catalogue number GB 11233-service bio-USA). The process was conducted by the labeled streptavidin–biotin complex procedure [25]. Firstly, the tissues were embedded in paraffin. Then, they were mounted on poly-L-lysine coated glass slides, sections were 3–4-µm- in thickness. After that, specimens were deparaffinized by putting them in xylene for ten minutes. Then dehydrated in a graded series of ethanol alcohol. Unmasking of the antigenic sites was done by placing the sections in the microwave in 0.01 citrate buffer concentration for 10 min in formalin-fixed tissues and to enhance the stainability of the primary antibody. The sections were further treated with 0.3% hydrogen peroxide in phosphate-buffered solution (PBS) (100 µL) for 10 min at room temperature to achieve endogenous peroxidase blocking. Finally, the sections were incubated with the primary antibody for one hour at room temperature, followed by incubation in biotinylated secondary antibody in PBS for 30 min at room temperature and subsequently with streptavidin–peroxidase conjugate.

The peroxidase activity was visualized by the chromogen diaminobenzidine hydrochloride. Mayer's Hematoxylin was used to counterstain the sections. A negative control for each reaction was obtained by omitting the primary antibody.

Analysis of IHC staining:

The area percent for osteocalcin immune reactivity was calculated for each group considering the area percentage. Cells were deemed positive without considering the staining intensity. The number of positive cells was computed by checking five different fields in the microscope with magnification (×400). Immuno-reactivity mean area fraction (MAF) was calculated using ImageJ 1.46 r software [26].

Statistical analysis

With the use of the IBM SPSS software package version 20.0, data were input into the computer and analyzed. (IBM Corp, Armonk, NY). The normality of continuous data was determined using Shapiro-Wilk test. For quantitative normally distributed variables, mean, range (minimum and maximum), and standard deviation were used to present quantitative data. The three study groups were compared using the one-way ANOVA test, and Tukey's Post Hoc test was used to compare each two groups pairwise. At the five percent level, the significance of the results was determined.

RESULTS

BM-MSC Immunophenotyping

Flow cytometry analysis (FACs caliber, BD) for BM-MSC at P3 revealed: 97.30 percent of cultured cells expressed CD90 mesenchymal marker while being negative for the hematopoietic CD45 marker (Figure 2a). The mesenchymal CD44 marker was expressed in 98.49% of cultured cells (Figure 2b). and 96.85 % expressed the mesenchymal CD73 marker (Figure 2c). The mesenchymal CD105 markers and CD11b were expressed by cultured cells at the percentages of 97.36 % and 1.98% respectively (Figures 2d, e).

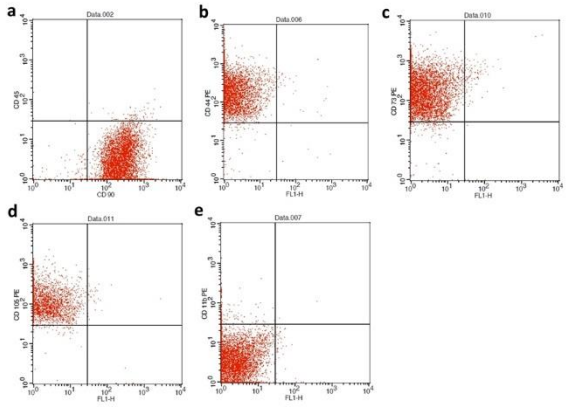

Figure (2): Flow cytometry analysis for BM-MSCs cell surface markers at P3 showing (a) 97.30% of cultured cells expressed CD90 mesenchymal marker in the lower-right quadrant; however, they were negative for CD45 hematopoietic marker in the upper-left quadrant. (b-e) percentages of mesenchymal markers CD44, CD73, CD105, and CD11b expressed by cultured cells as 98.49, 96.85, 97.36, and 1.98 % respectively the upper-left quadrant.

Characterization of extracellular vesicles

In vitro characterization of exosomes using Zeta sizer and TEM

Particle size analysis of isolated exosomes showed a size of 78.8 nm with a narrow PDI of 0.3 with a negative zeta-potential of -28 ± 154 mV confirming their colloidal stability (Figure 3a). The morphological analysis by TEM revealed rounded extracellular vesicles with variable size range 32.72- 48.22 nm (Figure 3b).

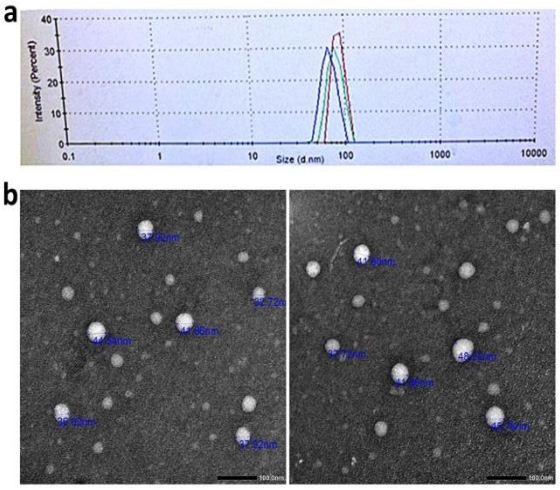

Figure (3): (a) Zeta sizing (b) TEM showing isolated EVs with different sizes ranging from 32.72- 48.22 nm, scale bar; 100 nm.

BCA protein assay for exosomes quantification

It demonstrated that the concentration of proteins was 800 ug/mL, reflecting an increased concentration of EVs and the efficient isolation process.

Characterization of collagen thermoresponsive hydrogels

3.1 Investigation of Gelation Behavior

The temperature that exosome-loaded and unloaded collagen hydrogels were subjected to varied in the gelation time. Both thermo-responsive formulas didn't form a gel at four degree- centigrade. At room temperature (twenty-five degree-centigrade), the exosome-loaded and unloaded Collagen hydrogels gelation time were 125 and 100 seconds subsequently. It was decreased from 125 to 45 seconds and from 100 to 30 seconds for exosome-loaded and unloaded collagen hydrogels when subjected to thirty-seven degree-centigrade. Pluronic F-127 presented in the monomer form in the solution at 4°C. With increasing the tepmrature to 25°C, equality among micelles and monomers is achieved, where at elevated temperatures, an increase in viscosity and gel formation occurs owing to the formation of aggregates [27] .

Swelling ratio (SR):

SR as a function of time for exosome-loaded and unloaded collagen thermo-responsive gels was presented in Figure 3b. It was noted that the unloaded collagen gel has absorbed more water initially than the exosome-loaded collagen gel. The highest SR was demonstrated up to 24h. It was found that expanding the time caused higher gel swelling.

Viscosity measurement

The change in viscosity at different temperatures for the formed thermo-responsive gels is presented in Table (1).

Table (1): Viscosity (in centipoise) of unloaded and exosomes-loaded collagen thermoresponsive gel at different temperatures (4, 25, and 37oC)

	4oC	25oC	37oC
Unloaded collagen gel	1,265	22,780	66,010
Exosome-loaded collagen gel	985	11,030	39,500

Light microscopic results

Coll- group after 4 Weeks

Histological picture of the H&E-stained defects grafted with collagen hydrogel revealed a central filling of dispersed widely separated trabeculae of newly formed bone of variable thickness. The maturation of bone in focal zones was evidenced by the appearance of primary osteons. However, persistent wide immature islands of woven bone characterized by numerous wide osteocytes lacunae were also noticed. A well-vascularized ectomesenchymal tissue was also displayed. Remnants of the hydrogel droplets were also observed in between the bony segments (Figure 4a-c, Figure 5a-c).

Coll + Exos group after 4 Weeks

The bone defects loaded with collagen + exosomes presented a bridge of interconnected well organized parallel trabeculae of new bone. The nature of bone showed a more mature architecture reflected by the parallel lamellae of primary osteons, normal-sized osteocytes, and nutritive canals. The remains of hydrogel droplets were similarly revealed. The outer and inner circumferential lamellae were also noticed to start their formation and arrangement (Figure 4 d-f, Figure 5d-f).

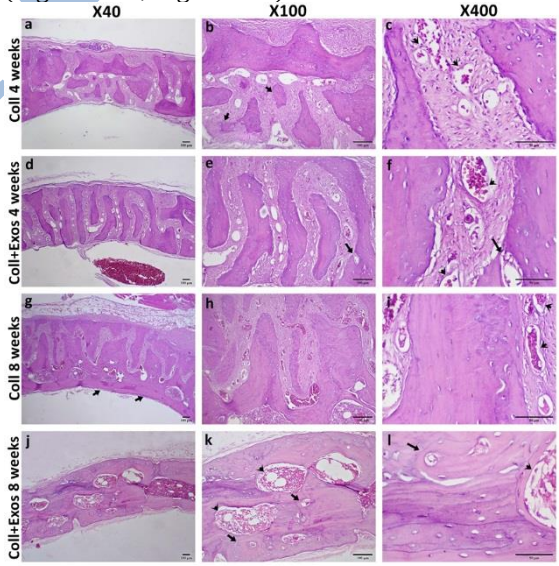

Figure (4): (a-c) showing Coll-group after 4 weeks revealing a central filling of dispersed widely separated trabeculae of newly formed bone and early primary osteons. Wide islands immature of woven bone (black arrows) with numerous wide osteocytes lacunae. Rich vascularity was also displayed (arrowheads). Remnants of the hydrogel

droplets appeared as white spaces in between bony segments. (a X40, b X100, c X400); (d-f) Coll + Exos group after 4 weeks presenting a bridge of interconnected well-organized parallel trabeculae of new bone. Mature parallel lamellae, normal-sized osteocytes, and nutritive canals (arrows). The remains of hydrogel droplets were similarly revealed, noting rich vascularity (arrowheads) (d X40, e X100, f X400); (g-i) Coll- group after 8 weeks showing parallel inner circumferential lamellae (arrow) of compact bone bridging one side of the defect. Interconnected trabeculae of the mature spongy bone surrounding a pronounced vasculature were also noted (arrowheads) (g X40, h X100, i X400); (j-l) Coll + Exos group after 8 weeks displaying a well-organized mature configuration of outer and inner plates surrounding a bony core divided into compact osteons (arrows) and trabeculae of lamellar cancellous bone. Highly cellular bone marrow cavities (arrowheads) were also shown comprising myeloid tissue (j X40, k X100, l X400) [H&E; Scale bar 100 & 50 µm].

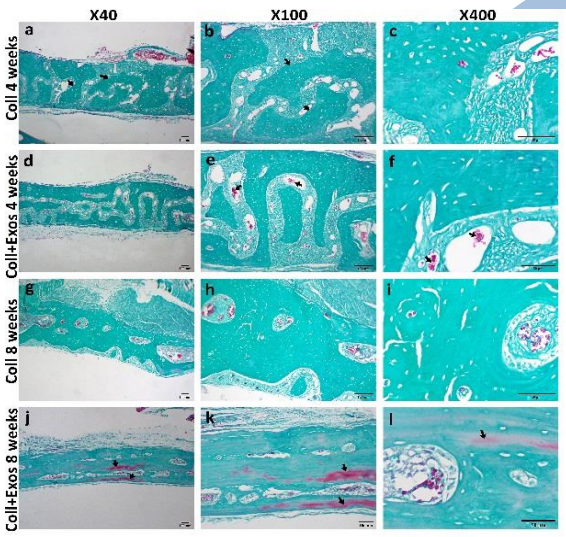

Figure (5): (a-c) Coll-group after 4 weeks showing thick separated trabeculae of newly formed bone surrounded by remnants of the hydrogel droplets (arrows) (a X40, b X100, c X400); (d-f) Coll + Exos group after 4 weeks presenting a bridge of interconnected well-organized trabeculae of new bone with mature parallel lamellae surrounded by the remains of hydrogel droplets, note rich vascularity (arrows) and the start of arrangement of inner and outer circumferential lamellae(d X40, e X100, f X400); (g-i) Coll- group after 8 weeks showing compact bony areas were also evidenced with well-arranged lamellae of inner and outer cortices starting to form (g X40, h X100, i X400); (j-l) Coll + Exos group after 8 weeks displayed a well-organized mature configuration of outer and inner plates surrounding a lamellar bony core bone. Note spots of highly mineralized bone stained in red (arrows) (j X40, k X100, l X400) [Trichrome; Scale bar 100 & 50 µm].

Coll- group after 8 weeks

The collagen-loaded sites after 8 weeks showed interconnected trabeculae of the mature spongy bone surrounding a pronounced vasculature. Parallel inner circumferential lamellae of compact bone bridging one side of the defect (Figure 4g-i). Compact bony areas were also evidenced with well-arranged lamellae of inner and outer cortices starting to form (Figure 5g-i).

Coll + Exos group after 8 weeks

The collagen + exosomes group was associated with a well-organized mature configuration of outer and inner cortical plates surrounding a bony core divided into compact osteons and trabeculae of lamellar cancellous bone. Highly cellular bone marrow cavities were also shown comprising myeloid tissue (Figure 4j-l). The lamellar configuration of bone was revealed associated with rich vascularity (Figure 5j-l).

Histomorphometric results

Quantitative evaluation of the newly formed bone filling the critical size defect created by measuring the area percent of new bone is presented in Table 2. After 4 weeks, the area percent of new bone showed higher values in the Exos group compared to the Coll group (mean = 69.51 and 54.31 respectively) with a significant difference (P2=0.013); however, after 8 weeks no significant difference was detected (P5=0.933). Moreover, the percent of new bone in the Coll group increased significantly from 4 to 8 weeks (mean = 54.31 and 67.72 respectively; P1=0.033); although no significant difference was found in the Exos group upon the same interval (mean=69.51 and 70.5 respectively; P6=0.997).

Table (2): Area percent of newly formed bone among groups

SD: Standard deviation

	COLL 4 weeks (n = 10)	COLL 8 weeks (n = 10)	COLL+EXOS weeks (n = 10)	COLL+EXOS weeks (n = 10)	F	p
Area % of newly formed bone						
Min. – Max.	36.21 – 69.88	49.41 – 82.77	57.94 – 82.35	53.61 – 89.02	5.220*	0.004*
Mean ± SD.	54.31b ± 11.23	67.72a ± 10.38	69.51a ± 8.19	70.50a ± 11.67		
	p1=0.033*,p2=0.013*,p3=0.007*,p4=0.980,p5=0.933,p6=0.997					

F: F for One-way ANOVA test, pairwise comparisons were done using Post Hoc Test (Tukey)

p: p-value for comparing the four studied groups

p1: p-value for comparing between COLL 4 weeks and COLL 8 weeks

p2: p-value for comparing between COLL 4 weeks and COLL+EXOS 4 weeks

p3: p-value for comparing between COLL 4 weeks and COLL+EXOS 8 weeks

p4: p-value for comparing between COLL 8 weeks and COLL+EXOS 4 weeks
p5: p-value for comparing between COLL 8 weeks and COLL+EXOS 8 weeks
p6: p-value for comparing between COLL+EXOS 4 weeks and COLL+EXOS 8 weeks
*: Statistically significant at $p \leq 0.05$
Means with any Common letter (a-b) are not significant

Immunohistochemical results

Immunohistochemical evaluation revealed that the highest area percent for osteocalcin expression was presented in the Exos group after 4 weeks (197.5) compared to the Coll group on the same time interval (22.66). After 8 weeks, the area percent for osteocalcin immuno- expression revealed higher values in the Exos group compared to the Coll group (mean = 112.2 and 194.9 respectively); however, after 8 weeks no significant difference was detected (P5=0.914). Moreover, the percent of new bone in the Coll group increased significantly from 4 to 8 weeks (mean = 22.66 and 104.9 respectively; P1 < 0.001). A significant difference was also found in the Exos group upon the same interval (mean=197.5 and 112.2 respectively; P6< 0.001). These results were tabulated in Table (3) and seen in Figure (6).

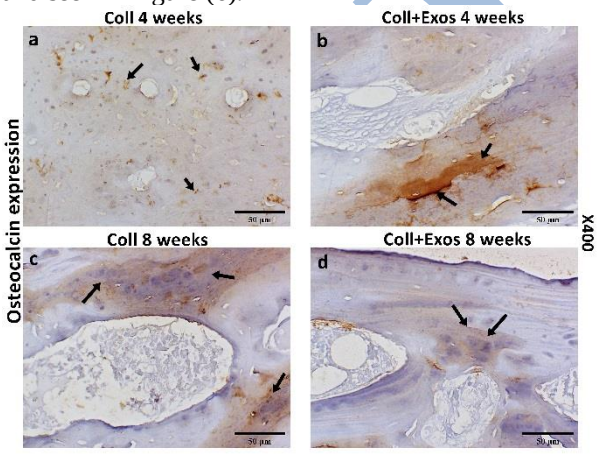

Figure (6): Osteocalcin immunoexpression in the 4 different groups (a) Coll-group after 4 weeks showing sporadic osteocalcin immune signals in the osteocytes(arrows) (x400). (b) Coll + Exos group after 4 weeks presenting more dense well-organized new bone exhibiting brown positive immune signals sporadically intranuclear in the osteoblasts (arrows) and in the bone matrix (x400) (c) Coll after 8 weeks showing positive immunoexpression for osteocalcin omitting the bone marrow spaces and mainly in the bone matrix membranous reaction (arrows) (x400). (d) Coll+ Exos group after 8 weeks showing compact bony areas showing concentric lamellar brown lines positive for osteocalcin (arrows). (x400)

Table (3): Osteocalcin Immuno-expression among the Different Groups

	COLL 4 weeks (n = 10)	COLL 8 weeks (n = 10)	COLL+EXOS 4 weeks (n = 10)	COLL+EXOS 8 weeks (n = 10)	F	p
Area percent of Osteocalcin immunoexpression						
Min. – Max.	13.30 – 29.33	72.24 – 145.7	151.6 – 251.8	87.43 – 159.5	0.289*	<0.001*
Mean ± SD.	22.66c ± 4.59	104.9b ± 23.70	197.5a ± 38.58	112.2b ± 21.74		
	p1<0.001*,p2<0.001*,p3<0.001*,p4<0.001*,p5=0.914,p6<0.001*					

SD: Standard deviation
F: F for One way ANOVA test, Pairwise comparisons were done using Post Hoc Tukey Test
p: p-value for comparing the four studied groups
p1: p-value for comparing between COLL 4 weeks and COLL 8 weeks
p2: p-value for comparing between COLL 4 weeks and COLL+EXOS 4 weeks
p3: p-value for comparing between COLL 4 weeks and COLL+EXOS 8 weeks
p4: p-value for comparing between COLL 8 weeks and COLL+EXOS 4 weeks
p5: p-value for comparing between COLL 8 weeks and COLL+EXOS 8 weeks
p6: p-value for comparing between COLL+EXOS 4 weeks and COLL+EXOS 8 weeks
*: Statistically significant at $p \leq 0.05$
Means with any Common letter (a-b) are not significant

DISCUSSION

Rat calvaria was found to be commonly operated upon as it strongly relates the experimental studies to the clinical ones [28]. As a result, rat calvaria were chosen to be used in this study to match as much as possible the results most relevant to the human bone regeneration process.

A critical-size defect (CSD) can be defined as one that fails to heal freely within the period of the study [28-30]. Therefore, in this study, a CSD of size 6mm was performed, which is considered suitable for the chosen young age of the rats utilized. This was in agreement with Hatakeyama W. et al. who performed a 6 mm CSD in Wistar rats aged 10-week-old, which were implanted with P-nHAP/COL and pressed collagen (P-COL) [31].

The chosen follow-up periods in this study were 4 and 8 months. These periods were considered to be long enough to evaluate the healing process and tissue regeneration in the rat models. Moreover, it was always a motivation for researchers in the medical field as well as dentists to seek the shortest follow-up periods in materials used in osseous regeneration for their patients' benefit [32].

The rats were included in the current study because of their close similarity to humans anatomically,

physiologically, and genetically. Moreover, their availability, low cost, and relatively longer life span than other animals [33]. This was in accordance with Costa et al. [28], who used rodents to investigate bone regeneration. In addition, they found that rodents are utilized for in vivo bone therapy and regeneration. Moreover, there are different ways to isolate the EVs; but, the differential ultra-centrifugation was a successful method to isolate EVs, and to remove the large apoptotic bodies.

EVs vary in size (30 to 150 nm) and diameter. They are specialized by their unique lipids, proteins, micro-RNA, DNA, and enzymes components. The molecular composition of the EVs varies depending on the cell's place of origin. They are also signal-related organelles that are made by a variety of cell types. Exosomes, microvesicles, and apoptotic bodies are examples of membrane-bound vesicles that are produced by both healthy and dying cells and by all species. Extracellular vesicles are classified according to their size (exosomes are between 40 and 100 nm, bigger microvesicles are between 100 and 500 nm, and apoptotic bodies are between 500 and 2 nm) [34]. Extracellular vesicles serve a variety of purposes, including those of a medication delivery system, diagnostic tool, immunological response, and wound healing [35].

This present study aimed at evaluating the effect of collagen hydrogel containing BMMSC-derived exosomes on bone regeneration in rat calvarial critical-size bone defect by histological, immunohistochemical, and histomorphometric analysis.

TEM was utilized for extracellular vesicle characterization. It revealed that it was spherical in shape and its size ranged from 32.72- 48.22 nm. This comes in agreement with Van Der Pol et al. [36], who studied different methods for the characterization of micro-particles and exosomes; they found that extracellular vesicles are best seen with TEM because of its high-resolution capacity that can identify nano-sized particles; thus, it's an essential tool for characterizing the shape and size of exosomes.

Meanwhile, the protein content of extracellular vesicles was calculated using the BCA assay and it was 800 ug/mL, insuring the high protein content of EVs, and that isolation was done efficiently. These outcomes were online with Stillwell et al. [37], who investigated the biological membranes and proved that protein counts from 25–75 % of the weight of different biological membranes, where the majority of the membranes have about 50 % protein. In addition, Smyth et al. [38] illustrated that proteins play a vital role in the adherence and internalization of extracellular vesicles by the recipient cell.

Furthermore, Zeta sizing analysis illustrated that the largest size of the nanoparticles was 78.8 nm. These results were confirmed by Khodashenas et al. [39], as they investigated variable methods for characterizing extracellular vesicles for variable purposes.

Upon histological, histomorphometric, and immunohistochemical analysis, evidence of new bone filling the surgical defect created was revealed in both groups after 4 and 8 weeks. However, the quantity of bone measured as the surface area was enhanced significantly in the Coll+Exos group compared to the collagen hydrogel group. In addition, the quality of bone reflected a better maturation and organization in association with exosomes. These findings reflect that the addition of exosomes to the collagenous scaffold not only promoted bone formation but accelerated osteoblastic differentiation. Our observation also denoted the noticeable rich vascular supply provided in the Coll+Exos group. However, there was no significant difference between the Coll group and Coll+ Exo group at 8 weeks. The could be explained by that the BMMSC-derived exosomes enhanced the proliferation and osteogenic differentiation, in calvarial defects, so bone regeneration was markedly accelerated in rats treated with BMMSC-derived exosomes in 4 weeks but the longer duration (week 8) gave chance for osteogenic differentiation in presence of the collagen hydrogel thus both groups were comparable to each other(1). Similar results were reported by Takeuchi et al. [12], who revealed that after 4 weeks of implantation of BMMSC-derived exosomes embedded in an atelocollagen scaffold sponge, a maturing bony bridge was evident with enhanced expression of osteocalcin marker of bone formation and Vascular endothelial growth factor (VEGF) marker of angiogenesis. Similarly, Zhang et al. [40] also demonstrated that BMMSC promoted osteogenesis in a rat model of fracture non-union through the upregulation of RUNX2, OSP, and OCN markers of bone formation in comparison to the exosome-free group. Moreover, the in vitro experiment of the same study showed that the osteogenic differentiation mediated by exosomes depends on the BMP-2/Smad1/RUNX2 signaling pathway [40]. Liang et al. [41] also revealed that the injection of BMMSC-derived exosomes in calvarial bone defect increased bone formation and increased new vessel formation upregulation CD31. The new bone formation noted by osteocalcin expression in the exosomes group was supported by the study by Ying C et al. [42] that concluded that MSC carry special mutant which is hypoxia-inducible factor 1 (HIF-1) which is responsible for neovascularization and osteogenesis in critical sized bone defect. Our results go with Huang Y et al. research [43] that revealed that bone marrow mesenchymal exosomes showed increased osteocalcin activity in a model of osteoarthritis as

our results showed higher osteocalcin expression with adding exosomes with collagen.

The addition of exosomes also promoted endothelial cell division and migration when tested in vitro compared to the control group [41]. Through the same mechanism of action, BMMSC derived-exosomes induced bone-tendon healing in the rotator cuff of rat models [44]. Furthermore, Jia et al. reported an increased callus formation and consolidation upon the implantation of exosomes derived from young BMMSC during tibial distraction osteogenesis where, distraction osteogenesis is a clinically effective procedure to regenerate large bone defects [45].

Additionally, loading scaffolds with exosomes, of BMMSC origin, resulted in superior bone healing compared to the β-TCP scaffold group in CSD of calvaria [46].

The osteogenic potential of Exosomes derived from the healthy BMMSCs is referred to as the suppression of the adipogenic differentiation pathway, which in turn favors the osteogenic differentiation. Another reason is that BMMSC-derived exosomes express key proteins of the bone-forming MAPK signaling pathway, stimulating osteoblastic proliferation and decreasing apoptosis [47].

The current work illustrated exclusively that collagen hydrogel loaded by BMMSCs-derived exosomes not only promotes but accelerates bone regeneration in calvarial critical-sized bone defects. Therefore, the application of exosome-based bone engineering might be a favorable option substituting cell-based therapies and the associated drawbacks.

Abbreviations:

(BM-MSCs) Bone marrow-derived mesenchymal stem cells
(BMP-2) Bone morphogenetic protein - 2
(BSP) bone sialoprotein
(CERRMA) Center of excellence for research in regenerative medicine and its application
(COLL) Collagen hydrogel
(CSD) Critical-size defect
(DMEM) Dulbecco's Modified Eagle Medium
(EDTA) Ethylene diamine tetra-acetic acid
(EVs) Extracellular vesicles
(FBS) Fetal bovine serum
(mAb) Monoclonal antibodies
(MAPK) Mitogen-activated protein kinase
(MAF) Mean area fraction
(miRNA) microRNA
(MSCs) Mesenchymal stem cells
(OCN) Osteocalcin
(OSP) Osteopontin
(PASS) Power analysis and sample size software
(PBS) Phosphate buffer saline
(PE) Phycoerythrin
(RPM) Revolutions per minute
(RUNX-2) Runt-related transcription factor 2
(Smad1) Suppressor of Mothers against Decapentaplegic (receptor of bone morphogenic protein)
(B-TCP) Beta tricalcium phosphate

Declarations

Author contributions

Sara A. Hamza: conceptualization, methodology, validation, data curation, investigation, resources, writing-original -original draft preparation, visualization, and writing-reviewing and editing. Marwa Gamal Noureldin; methodology- surgical procedures, interpretation, resources, writing-original -original draft preparation – Lamia Ahmed Heikal: methodology – hydrogels preparation and characterization, resources writing-, - Enas Magdi Omar: Methodology – immunohistochemical analysis, writing- Hagar Sherif Abdel Fattah: conceptualization, methodology, validation, data curation, investigation, resources, writing-original -original draft preparation, visualization, and writing-reviewing and editing.

Funding

The authors received no specific funding for the study.

Availability of data and materials

All datasets and materials used and/or analyzed during the current study are included in this published article.

Ethics approval and consent to participate

The proposal of the presented work was approved by the institutional Research Ethics Committee of the Faculty of Dentistry, Alexandria University, Egypt (IORG 0008839). The current study conforms to the ARRIVE guidelines.

Consent to participate

Not applicable.

Consent for publication

Not applicable.

Competing interests

The authors declare no competing interests.

Acknowledgments

The authors are grateful to the Center of Excellence for Research in Regenerative Medicine and Applications (CERRMA), Faculty of Medicine, Alexandria University (STDF-Funded) for the assistance provided by the staff and especially thanks to Prof. Radwa Mehanna. Also, we extend our thanks to the staff in the Animal House, Faculty of Medicine, Alexandria University for their professional academic handling of the rats.

REFERENCES

1. Zhou, J., et al., Biomaterials and nanomedicine for bone regeneration: Progress and future prospects. Exploration (Beijing), 2021. 1(2): p. 20210011.
2. Shang, F., et al., Advancing application of mesenchymal stem cell-based bone tissue regeneration. Bioact Mater, 2021. 6(3): p. 666-683.

3. Hinsenkamp, M., et al., Adverse reactions and events related to musculoskeletal allografts: reviewed by the World Health Organisation Project NOTIFY. Int Orthop, 2012. 36(3): p. 633-41.
4. Stamnitz, S. and A. Klimczak, Mesenchymal Stem Cells, Bioactive Factors, and Scaffolds in Bone Repair: From Research Perspectives to Clinical Practice. Cells, 2021. 10(8).
5. Røsland, G.V., et al., Long-term cultures of bone marrow-derived human mesenchymal stem cells frequently undergo spontaneous malignant transformation. Cancer Res, 2009. 69(13): p. 5331-9.
6. Volarevic, V., et al., Ethical and Safety Issues of Stem Cell-Based Therapy. Int J Med Sci, 2018. 15(1): p. 36-45.
7. Sui, B.D., et al., Stem cell-based bone regeneration in diseased microenvironments: Challenges and solutions. Biomaterials, 2019. 196: p. 18-30.
8. Tan, S.H.S., et al., Mesenchymal stem cell exosomes in bone regenerative strategies-a systematic review of preclinical studies. Mater Today Bio, 2020. 7: p. 100067.
9. Tang, Y., Y. Zhou, and H.J. Li, Advances in mesenchymal stem cell exosomes: a review. Stem Cell Res Ther, 2021. 12(1): p. 71.
10. Mendt, M., K. Rezvani, and E. Shpall, Mesenchymal stem cell-derived exosomes for clinical use. Bone Marrow Transplant, 2019. 54(Suppl 2): p. 789-792.
11. Hade, M.D., C.N. Suire, and Z. Suo, Mesenchymal Stem Cell-Derived Exosomes: Applications in Regenerative Medicine. Cells, 2021. 10(8).
12. Takeuchi, R., et al., Exosomes from conditioned media of bone marrow-derived mesenchymal stem cells promote bone regeneration by enhancing angiogenesis. PLoS One, 2019. 14(11): p. e0225472.
13. Kanbur, N.O., et al., Osteocalcin. A biochemical marker of bone turnover during puberty. Int J Adolesc Med Health, 2002. 14(3): p. 235-44.
14. Percie du Sert, N., et al., The ARRIVE guidelines 2.0: Updated guidelines for reporting animal research. Br J Pharmacol, 2020. 177(16): p. 3617-3624.
15. Wang, L., et al., A New Self-Healing Hydrogel Containing hucMSC-Derived Exosomes Promotes Bone Regeneration. Front Bioeng Biotechnol, 2020. 8: p. 564731.
16. Muralidharan, K., Six Sigma for Organizational Excellence: A Statistical Approach. 2015.
17. Abolgheit, S., et al., Bone marrow-derived mesenchymal stem cells and extracellular vesicles enriched collagen chitosan scaffold in skin wound healing (a rat model). J Biomater Appl, 2021. 36(1): p. 128-139.
18. Thabet, E., et al., Extracellular vesicles miRNA-21: a potential therapeutic tool in premature ovarian dysfunction. Mol Hum Reprod, 2020. 26(12): p. 906-919.
19. Xu, R., et al., Extracellular vesicle isolation and characterization: toward clinical application. J Clin Invest, 2016. 126(4): p. 1152-62.
20. Ghanem, M., et al., The Effect of Coenzyme Q10/Collagen Hydrogel on Bone Regeneration in Extraction Socket Prior to Implant Placement in Type II Diabetic Patients: A Randomized Controlled Clinical Trial. J Clin Med, 2022. 11(11).
21. Yang, J., et al., Umbilical Cord-Derived Mesenchymal Stem Cell-Derived Exosomes Combined Pluronic F127 Hydrogel Promote Chronic Diabetic Wound Healing and Complete Skin Regeneration. Int J Nanomedicine, 2020. 15: p. 5911-5926.
22. Hudieb, M., et al., Influence of Age on Calvarial Critical Size Defect Dimensions: A Radiographic and Histological Study. J Craniofac Surg, 2021. 32(8): p. 2896-2900.
23. Kumar, G., Orban's Oral Histology & Embryology-E-BOOK. 2015: Elsevier Health Sciences.
24. Melsen, F. and T. Steiniche, Bone histomorphometry. Osteoporos Int, 1993. 3 Suppl 1: p. 98-9.
25. Magaki, S., et al., An Introduction to the Performance of Immunohistochemistry. Methods Mol Biol, 2019. 1897: p. 289-298.
26. WS, R., Imagej, us national institutes of health, bethesda, maryland, usa. http://imagej. nih. gov/ij/, 2011.
27. Lupu, A., et al., Temperature Induced Gelation and Antimicrobial Properties of Pluronic F127 Based Systems. Polymers, 2023. 15(2): p. 355.
28. Souza, E.Q.M., et al., Evaluations of hydroxyapatite and bioactive glass in the repair of critical size bone defects in rat calvaria. J Oral Biol Craniofac Res, 2020. 10(4): p. 422-429.
29. Lohmann, P., et al., Bone regeneration induced by a 3D architectured hydrogel in a rat critical-size calvarial defect. Biomaterials, 2017. 113: p. 158-169.
30. Piotrowski, S.L., et al., Development and Characterization of a Rabbit Model of Compromised Maxillofacial Wound Healing. Tissue Eng Part C Methods, 2019. 25(3): p. 160-167.
31. Hatakeyama, W., et al., Bone Regeneration of Critical-Size Calvarial Defects in Rats Using Highly Pressed Nano-Apatite/Collagen Composites. Materials (Basel), 2022. 15(9).
32. Cooper, G.M., et al., Testing the critical size in calvarial bone defects: revisiting the concept of a critical-size defect. Plast Reconstr Surg, 2010. 125(6): p. 1685-1692.

33. Bryda, E.C., The Mighty Mouse: the impact of rodents on advances in biomedical research. Mo Med, 2013. 110(3): p. 207-11
34. Battistelli, M. and E. Falcieri, Apoptotic Bodies: Particular Extracellular Vesicles Involved in Intercellular Communication. Biology (Basel), 2020. 9(1).
35. van Niel, G., et al., Exosomes: a common pathway for a specialized function. J Biochem, 2006. 140(1): p. 13-21.
36. Imanbekova, M., et al., Recent advances in optical label-free characterization of extracellular vesicles. Nanophotonics, 2022. 11(12): p. 2827-2863.
37. Stillwell, W., An introduction to biological membranes: from bilayers to rafts. 2013: Newnes.
38. Smyth, T.J., et al., Examination of the specificity of tumor cell derived exosomes with tumor cells in vitro. Biochim Biophys Acta, 2014. 1838(11): p. 2954-65.
39. Khodashenas, S., S. Khalili, and M. Forouzandeh Moghadam, A cell ELISA based method for exosome detection in diagnostic and therapeutic applications. Biotechnol Lett, 2019. 41(4-5): p. 523-531.
40. Zhang, L., et al., Exosomes from bone marrow mesenchymal stem cells enhance fracture healing through the promotion of osteogenesis and angiogenesis in a rat model of nonunion. Stem Cell Res Ther, 2020. 11(1): p. 38.
41. Liang, B., et al., Dimethyloxaloylglycine-stimulated human bone marrow mesenchymal stem cell-derived exosomes enhance bone regeneration through angiogenesis by targeting the AKT/mTOR pathway. Stem Cell Res Ther, 2019. 10(1): p. 335.
42. Ying, C., et al., BMSC-Exosomes Carry Mutant HIF-1α for Improving Angiogenesis and Osteogenesis in Critical-Sized Calvarial Defects. Frontiers in Bioengineering and Biotechnology, 2020. 8.
43. Huang, Y., et al., Bone marrow mesenchymal stem cell-derived exosomal miR-206 promotes osteoblast proliferation and differentiation in osteoarthritis by reducing Elf3. J Cell Mol Med, 2021. 25(16): p. 7734-7745.
44. Huang, Y., et al., Bone marrow mesenchymal stem cell-derived exosomes promote rotator cuff tendon-bone healing by promoting angiogenesis and regulating M1 macrophages in rats. Stem Cell Research & Therapy, 2020. 11(1): p. 496.
45. Jia, Y., et al., Exosomes Secreted by Young Mesenchymal Stem Cells Promote New Bone Formation During Distraction Osteogenesis in Older Rats. Calcif Tissue Int, 2020. 106(5): p. 509-517.
46. Zhang, J., et al., Exosomes/tricalcium phosphate combination scaffolds can enhance bone regeneration by activating the PI3K/Akt signaling pathway. Stem Cell Res Ther, 2016. 7(1): p. 136.
47. Al-Sowayan, B., F. Alammari, and A. Alshareeda, Preparing the Bone Tissue Regeneration Ground by Exosomes: From Diagnosis to Therapy. Molecules, 2020. 25(18).